PHYSICAL REVIEW B **89**, 140503(R) (2014)

Power-law-like correlation between condensation energy and superconducting transition temperatures in iron pnictide/chalcogenide superconductors: Beyond the BCS understanding

Jie Xing,[1] Sheng Li,[1] Bin Zeng,[2] Gang Mu,[2] Bing Shen,[2] J. Schneeloch,[3] R. D. Zhong,[3] T. S. Liu,[3,4] G. D. Gu,[3] and Hai-Hu Wen[1,*]

[1]*Center for Superconducting Physics and Materials, National Laboratory of Solid State Microstructures and Department of Physics, Nanjing University, Nanjing 210093, China*

[2]*National Laboratory for Superconductivity, Institute of Physics and National Laboratory for Condensed Matter Physics, Chinese Academy of Sciences, Beijing 100190, China*

[3]*Condensed Matter Physics and Materials Science Department, Brookhaven National Laboratory, Upton, New York 11973, USA*

[4]*School of Chemical Engineering and Environment, North University of China, Shanxi 030051, China*

(Received 17 February 2014; revised manuscript received 31 March 2014; published 16 April 2014)

Superconducting condensation energy $U_0^{\rm int}$ has been determined by integrating the electronic entropy in various iron pnictide/chalcogenide superconducting systems. It is found that $U_0^{\rm int} \propto T_c^n$ with $n = 3$–4, which is in sharp contrast to the simple BCS prediction $U_0^{\rm BCS} = 1/2 N_F \Delta_s^2$, with N_F the quasiparticle density of states at the Fermi energy and Δ_s the superconducting gap. A similar correlation holds if we compute the condensation energy through $U_0^{\rm cal} = 3\gamma_n^{\rm eff}\Delta_s^2/4\pi^2 k_B^2$, with $\gamma_n^{\rm eff}$ the effective normal state electronic specific heat coefficient. This indicates a general relationship $\gamma_n^{\rm eff} \propto T_c^m$ with $m = 1$–2, which is not predicted by the BCS scheme. A picture based on quantum criticality is proposed to explain this phenomenon.

DOI: 10.1103/PhysRevB.89.140503 PACS number(s): 74.70.Dd, 74.40.Gh, 74.55.+v

Superconductivity is induced by quantum condensation of a large number of paired electrons, namely, the Cooper pairs. According to the Bardeen-Cooper-Schrieffer (BCS) theory, the pairing is supposed to be established between the two electrons with opposite momentum and spins by exchanging phonons. The formation of the electronic paired state will lower the total energy, leading to the condensation of the Cooper pairs. The condensation energy, defined as the difference of the Gibbs free energy of the system in the normal state and superconducting state, is given by $U_0^{\rm BCS} = 1/2 N_F \Delta_s^2$, with N_F the quasiparticle density of states (DOS) at the Fermi energy of the normal state and Δ_s the superconducting gap. Supposing a simple and natural relation $\Delta_s \propto T_c$, we have $U_0^{\rm BCS} \propto N_F T_c^2$. Normally N_F is weakly related to the superconducting gap Δ_s through $N_F = 1/V \ln[(2\hbar\omega_D)/\Delta_s]$, with V the attractive potential between the two electrons when exchanging a phonon and ω_D the Debye frequency, thus one can roughly expect that $U_0^{\rm BCS} \propto T_c^2$ in a conventional BCS superconductor.

Since the discovery of iron-based superconductors, the pairing mechanism still remains unresolved. One type of picture assumes a scenario similar to the BCS but using antiferromagnetic spin fluctuations as the pairing glue [1–4]. This is called the weak coupling approach. Another more exotic picture, based on the strong coupling approach, assumes the local magnetic interaction as the pairing force which simultaneously causes the pairing of two electrons [5–8]. However, both pictures will ultimately lead to an $s^{\pm}$ pairing gap as the natural one. Specific heat (SH) measurements are very powerful, not only for detecting the gap symmetry [9–11], but also in unraveling some deeper mysteries related to the superconducting mechanism. For example, it was found by Bud'ko, Ni, and Canfield (BNC) [12] that, in the 122 systems, there is a simple scaling relation $\Delta C|_{T_c} \propto T_c^3$, with $\Delta C|_{T_c}$ the SH anomaly (jump) at T_c. This simple relation was later proved and solidified by further measurements with the samples experiencing different thermal treatments and annealing [13], and also extended to the 11 and 111 systems [14,15]. This $\Delta C|_{T_c} \propto T_c^3$ relation was explained as due to the impurity scattering effect in a multiband superconductor with an $s^{\pm}$ pairing gap [16]. However, this explanation may be challenged when making a comparison between $Ba_{1-x}K_xFe_2As_2$ and $Ba(Fe_{1-x}Co_x)_2As_2$: The former is much cleaner than the latter when judged through the residual scattering rate [17], but they follow a similar trend in the scaling relation $\Delta C|_{T_c} \propto T_c^3$. Another more novel picture, which is concerned with the quantum critical point (QCP) [18], was proposed to understand this interesting relation. Since the condensation energy is directly related to how much energy is saved when the system enters the superconducting state, thus it is highly desirable to have a systematic assessment of the condensation energy. In this Rapid Communication we try to calculate the condensation energy from ten pieces of our measured single crystals, and others from the published literature. Surprisingly, we discovered a simple power-law-like relation between the condensation energy and the superconducting transition temperatures.

Single crystals of $Ba_{1-x}K_xFe_2As_2$ ($x = 0.3, 0.4$), $Ba(Fe_{1-x}Co_x)_2As_2$, and $BaFe_{1.9}Ni_{0.1}As_2$ were grown by the flux method [9,19], and $FeSe_{0.5}Te_{0.5}$ by a unidirectional solidification method [20]. The SH data of $Ba_{1-x}K_xFe_2As_2$ ($x = 0.4$), $Ba(Fe_{1-x}Co_x)_2As_2$, and $BaFe_{1.9}Ni_{0.1}As_2$ single crystals were published in previous papers [9,19]. All doping concentrations of our samples are nominal ones. The SH measurements were done by the thermal relaxation method on the physical property measurement system (PPMS, Quantum Design) with an advanced measuring chip. For determining the condensation energy, we properly removed the phonon contributions (see below). We also obtained the electronic SH data from the published papers of other groups [11,21–32] so as to make the statistic results more convincing.

*hhwen@nju.edu.cn

 ©2014 American Physical Society

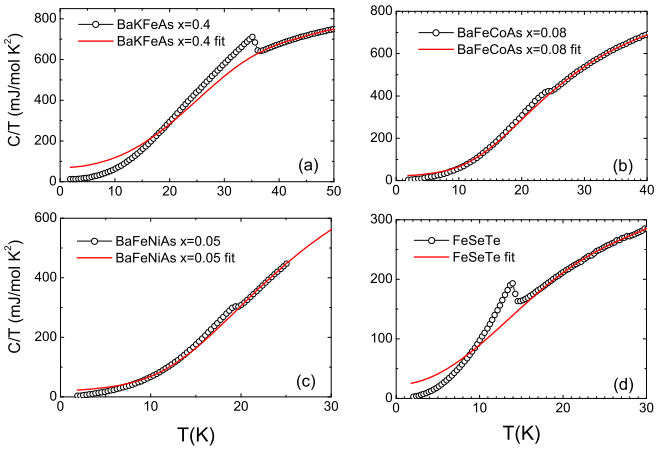

FIG. 1. (Color online) Raw data of SH for four different superconducting systems near the optimal doping point. The data are shown for samples (a) $Ba_{0.6}K_{0.4}Fe_2As_2$, (b) $Ba(Fe_{0.92}Co_{0.08})_2As_2$, (c) $BaFe_{1.9}Ni_{0.1}As_2$, and (d) $FeSe_{0.5}Te_{0.5}$. Here we show only four typical sets of data and the fitting curves of the normal state. More data are presented in the Supplemental Material.

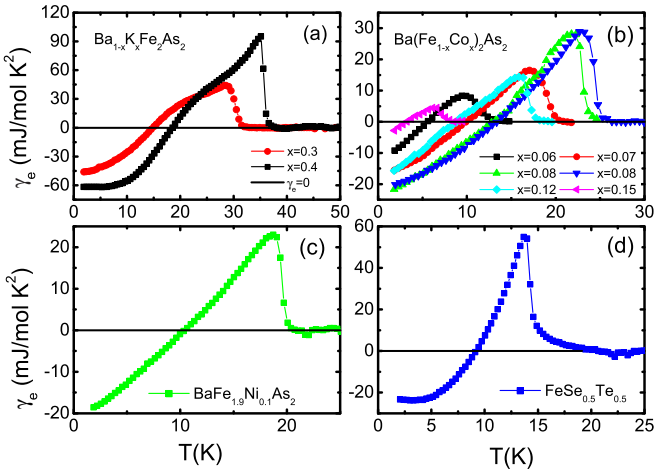

FIG. 2. (Color online) Temperature dependence of the superconducting electronic specific heat shifted by $\gamma_n^{\rm eff} + \gamma_0$, i.e., $C_e/T - \gamma_n^{\rm eff} - \gamma_0$ for (a) $Ba_{1-x}K_xFe_2As_2$, (b) $Ba(Fe_{1-x}Co_x)_2As_2$, (c) $BaFe_{1.9}Ni_{0.1}As_2$, and (d) $FeSe_{0.5}Te_{0.5}$.

In Fig. 1, we present the temperature dependence of SH for four of the ten typical samples. The sharp SH anomaly can be seen clearly at T_c for each sample. In order to obtain the electronic SH, we have to carefully investigate the phonon part of the total SH. For the $Ba(Fe_{1-x}Co_x)_2As_2$ and $BaFe_{1.9}Ni_{0.1}As_2$ samples, because the phonon contribution does not change much with doping, the overdoped nonsuperconducting samples are used as the references. Thus, from the formula

$$C_e^s(T) = C_{\rm total}^s(T) - pC_{\rm ph}^n(qT), \qquad (1)$$

we can derive the electronic term in each superconducting sample. Here $C_e^s(T)$ and $C_{\rm total}^s(T)$ are the electronic and total SH of the superconducting samples, respectively, and $C_{\rm ph}^n(T)$ is the phonon contribution of SH of the reference one. The p and q are fitting parameters which are determined by having a close matching effect of the phonon part between the superconducting sample and the reference one. It is found that p and q are close to 1 [19]. This slight modification of the phonon contribution is understandable since the doping may slightly change the lattice constants. For the $Ba_{1-x}K_xFe_2As_2$ and $FeSe_{0.5}Te_{0.5}$ samples, we use a polynomial function $C_{\rm nor} = C_e + C_{\rm ph} = \alpha T + \beta T^3 + \gamma T^5 + \cdots$ to fit the data in the normal state above T_c. In the fitting process, to ensure entropy conservation, we leave the electronic term α as the trial parameter which is manually adjusted and leave other higher-power temperature related terms totally free. The red lines in Fig. 1 show the phonon and the normal state electronic contribution of each sample. By using either a reference sample or the polynomial fitting method, one can find a good fit of the normal state of each superconducting sample. We must emphasize that the entropy conservation is a basic rule we hold in removing the phonon contribution in either of the methods mentioned above. This may inevitably lead to some uncertainties of the condensation energy with error bars of about $\pm 10\%$. For clarity, we only show data for four optimally doped samples in Fig. 1 and the data of the other six samples are presented in the Supplemental Material (SM) [33].

After subtracting the phonon contribution from the total SH, the electronic contribution is obtained for our ten samples, as shown in Fig. 2. The residual term at $T = 0$ K actually gives the effective SH coefficient $-\gamma_n^{\rm eff} = -[\gamma_n - \gamma(0)]$, with γ_n the total electronic SH of the normal state, including the nonsuperconducting term γ_0 [34]. The SH anomaly at T_c rises to a maximum at the optimal doping point with the highest T_c. Above T_c, the electronic SH decreases rapidly, except for $FeSe_{0.5}Te_{0.5}$. For $FeSe_{0.5}Te_{0.5}$, there is a tail extending up to a higher temperature, which has been found by other groups as well [21–24], but the cause remains unclear.

According to the BCS theory, the SH anomaly of a superconductor at T_c should follow $\Delta C/\gamma_n T_c = 1.43$ in the weak coupling limit. However, it was found that the iron-based superconductors severally violate this relation but show a simple correlation $\Delta C|_{T_c} \propto T_c^3$. This power law seems to be appropriate for many iron-based superconductors, with the majority of data so far for the 122 systems [12,14,15]. We also determined the SH anomaly of our ten samples and show them together with those of BNC in Fig. 3. Because of the finite width of the superconducting transition at T_c, we use the entropy conservation to determine the value of the SH anomaly and T_c in our samples. It is clear that our data fall onto the general power law $\Delta C|_{T_c} \propto T_c^3$ quite well, except for the $FeSe_{0.5}Te_{0.5}$ sample on which a deviation is observed. This may suggest that the general scaling law works better for one system, for example, for 122 here. However, we will show later that a scaling law of condensation energy with T_c seems more general to cover data from different systems, such as 122, 111, and 11.

Although a relation between $\Delta C|_{T_c}$ and the U_0 may be found based on the BCS picture [35], concerning the unconventional feature of superconductivity in iron-based superconductors, a detailed correlation between these two quantities is still lacking. Therefore it is worthwhile to determine the condensation energy independently. According

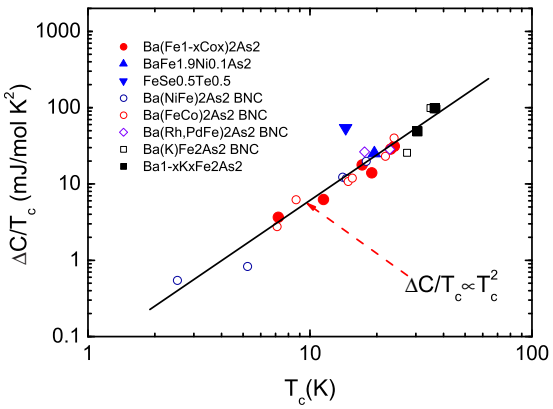

FIG. 3. (Color online) Correlations between the SH anomaly at T_c, i.e., $\Delta C/T_c|_{T_c}$ and T_c for many iron-based superconductors. The solid line shows the relationship with $\Delta C/T_c|_{T_c} \propto T_c^2$. The solid symbols are from our present experiment. The open ones are from the work of BNC.

to the thermodynamic definition, the entropy is $S = -\partial G/\partial T$, therefore we can calculate the condensation energy by integrating the entropy of the superconducting and normal state,

$$U_0^{\rm int} = \int_0^{T_c} [S_n(T) - S_s(T)]dT \tag{2}$$

$$= \int_0^{T_c} dT \int_0^{T} [C_n(T') - C_s(T')]/T'dT'. \tag{3}$$

The temperature dependence of entropy is shown in the SM for the four optimally doped samples. Because $[C_n(T) - C_s(T)]/T = \gamma_n(T) - \gamma_s(T)$, we can just compute the condensation energy with the electronic SH. We also calculate the condensation energy using the electronic SH data in previously published papers [11,21,22,25–32,36,37]. These data are plotted together with ours in Fig. 4(a). The dashed line shows the correlation $U_0^{\rm int} \propto T_c^{3.5}$. For different systems, the exponent n may vary a little, for example, for $Ba_{1-x}K_xFe_2As_2$, n is slightly smaller than that in $Ba(Fe_{1-x}T_x)_2As_2$ (T = Co and Ni). However, a global scaling law can be roughly satisfied with the exponent $n \approx 3$–4. Because the fermionic DOS should be weakly dependent on the doping level across the optimally doped point, the BCS theory implies that the condensation energy should scale roughly with T_c^2, which is very different from our result. We should mention that some published results from samples (mostly in the 111 system) with broad superconducting transitions are not included here. It is thus very curious to know whether more data points from a variety of systems are also obeying this scaling law. Furthermore, the SH data from the $K_xFe_{2-y}Se_2$ and KFe_2As_2 systems are not included. This is justified by the phase separation [38] in $K_xFe_{2-y}Se_2$. For the KFe_2As_2 system, the T_c is too low, which may prevent precisely determining the condensation energy [39].

Taking account of the BCS theory, we can deduce the condensation energy from the known values of $\gamma_n^{\rm eff}$ and the gap Δ_s as well. As a first approximation, assuming a spherical Fermi surface, the condensation energy is given by $U_0^{\rm cal} = 1/2N_F\Delta_s^2$ with the DOS $N_F = 3\gamma_n^{\rm eff}/(2\pi^2k_B^2)$ with

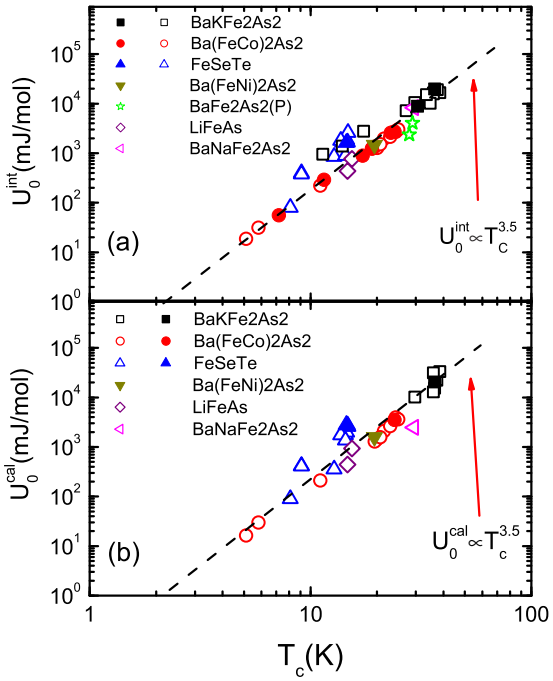

FIG. 4. (Color online) Correlations between the condensation energy and T_c in several iron-based systems. Here the condensation energy is calculated through (a) integrating the entropy in the superconducting state (see text) and (b) the simple computing formula $U_0^{\rm BCS} = 1/2N_F\Delta_s^2$. The dashed lines represent the relation $U_0^{\rm int}$ or $U_0^{\rm cal} \propto T_c^{3.5}$. Here the solid symbols are from our experiment, and the open ones are from the available literatures.

$\gamma_n^{\rm eff} = \gamma_n - \gamma_0$. From this argument, the condensation energy is derived as

$$U_0^{\rm cal} = \frac{3(\gamma_n^{\rm eff})}{4\pi^2k_B^2}\Delta_s^2. \tag{4}$$

Starting from above equation and the values of $\gamma_n^{\rm eff}$ and the gap, we calculate the condensation energy in an alternative way for our four optimally doped samples on which both the $\gamma_n^{\rm eff}$ and Δ_s are available, and from the published data for other samples [9,11,19,21,22,25–32]. Because of the multigap feature in the iron pnictide superconductors, some samples were fit by two s-wave gaps, so we used the average gap $\Delta_s = \sqrt{(p_1\Delta_1)^2 + (p_2\Delta_2)^2}$. For a d-wave component, the effective gap $\Delta_s = \frac{\sqrt{2}}{2}\Delta_d$ (here Δ_d is the maxima of the d-wave gap) is used in the formula. The calculated data of the condensation energy are plotted in Fig. 4(b). The dashed line shows the power law $U_0^{\rm cal} \propto T_c^{3.5}$. To our surprise, not only $U_0^{\rm int}$, but also the calculated value of the condensation energy $U_0^{\rm cal}$ obeys the correlation $U_0 \propto T_c^n$ with n of about 3–4. The result strongly indicates that the correlation between condensation energy and T_c reveals the intrinsic property in iron-based superconductors. If we look back to the BNC relation $\Delta C/T_c|_{T_c} \propto T_c^2$, a slight difference between our result and the BNC relation can be found by using the BCS theory. Taking $U_0^{\rm BCS} = 1/2N_F\Delta_s^2$, $\Delta_s = 1.75k_BT_c$, $N_F = 3\gamma_n^{\rm eff}/(2\pi^2k_B^2)$, we have $\Delta C|_{T_c} = 1.43\gamma_n^{\rm eff}T_c = 6.14U_0^{\rm BCS}/T_c$. This would suggest from our result that $\Delta C|_{T_c} \propto T_c^{2.5}$. This discrepancy further suggests that the simple BCS formulas,

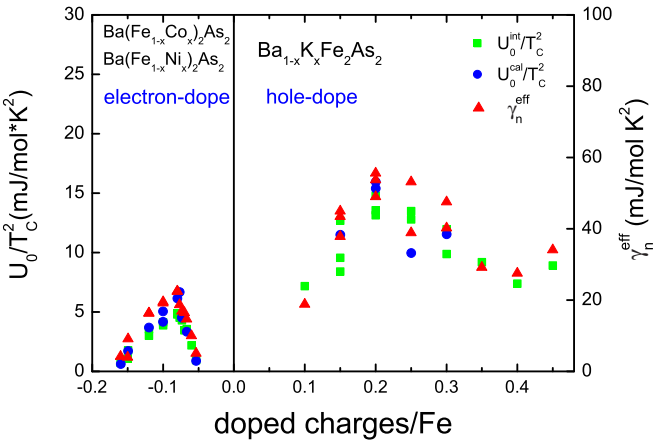

FIG. 5. (Color online) Doping dependence of $U_0^{\rm int}/T_c^2$, $U_0^{\rm cal}/T_c^2$, and $\gamma_n^{\rm eff}$ for electron doped and hole doped 122 samples. The three sets of data overlap each other.

especially those based on the weak coupling approach, cannot be used in the iron-based superconductors. Nevertheless, either the power-law-like relation found by BNC about the $\Delta C|_{T_c}$ vs T_c, or that between the condensation energy and T_c, are beyond the expectations of the BCS theory. In the following, we argue that the doping dependence of the effective DOS (or $\gamma_n^{\rm eff}$) may play an important role here.

Now we investigate the doping dependence of the condensation energy and the effective SH coefficient $\gamma_n^{\rm eff}$ in the 122 system. The results are shown in Fig. 5. It contains not only the data of our nine samples but also some available data from the literature. The x coordinate is the doped charges per Fe for every compound. In both doping sides, the quantities $U_0^{\rm int}/T_c^2$, $U_0^{\rm cal}/T_c^2$, and $\gamma_n^{\rm eff}$ overlap quite well and all exhibit a maximum around the optimal doping point. Taking account the result $U_0 \propto T_c^n$ with $n = 3$–4, we have $\gamma_n^{\rm eff} \propto T_c^m$ with $m = 1$–2. This is not expected by the BCS theory. Since $\gamma_n^{\rm eff}$ is closely related to the effective mass, we intend to argue that this doping dependence of $\gamma_n^{\rm eff}$ (or the effective DOS) results from the mass enhancement when it is around the quantum critical point (QCP).

As we know, the antiferromagnetism and superconductivity appear closely in the electronic phase diagram that is revealed either by doping or by applying a high pressure in iron-based superconductors. In most systems, if extrapolating the antiferromagnetic (AF) transition to zero temperature, it is found that the highest T_c appears near the point where the Néel temperature of the AF order becomes zero and a strong AF spin fluctuation emerges [40]. Near the optimal doping point, many novel electronic properties have been observed, for example, the penetration depth seems to have a singularity in the P-doped $BaFe_2As_2$ system [41]. Therefore it is quite possible that the effective mass of the electrons is strongly enhanced due to the strong coupling between the electrons and the AF spin fluctuations. This possible effect may bring about a power-law-like correlation between the condensation energy and T_c. It was also discovered that the enhancement of the effective mass appears near the quantum critical point in cuprates [42]. The divergent effective mass was found in the heavy fermion system near the antiferromagnetic quantum critical point as well [43]. Another feasible explanation which may be related to the above mentioned QCP mechanism is the small Fermi energy E_F in many iron-based superconductors. In the usual situation for the BCS picture, it is known that $\omega_D/E_F \ll 1$, and in this case the pair scattering occurs only near the very thin shell of the Fermi surface, while in the iron-based superconductors there are many shallow bands crossing the Fermi level, leading to a small Fermi energy E_F. This may further enhance the quantum fluctuation effect of the electronic system. Our observation here, that is, $U_0 \propto T_c^n$ with $n = 3$–4, can be explained as a consequence of the QCP as argued by Zaanen [18]. This will certainly stimulate further theoretical and experimental efforts on this general and interesting phenomenon.

In conclusion, the SH of many iron-based superconductors in the 122, 11, and 111 systems was investigated. From these data, we computed the condensation energy by two different methods and obtained similar power-law-like correlations $U_0^{\rm int} \propto T_c^n$ and $U_0^{\rm cal} \propto T_c^n$ with $n = 3$–4. Combining this relationship and the semiquantitative consideration of the BCS theory $U_0^{\rm BCS} = 1/2 N_F \Delta_s^2$, we find that the effective SH coefficient $\gamma_n^{\rm eff}$, or the effective DOS, is proportional to T_c^m with $m = 1$–2 across the doping regime, either in the electron or the hole doping side. All these power-law-like relations are beyond the BCS understanding, but can be explained based on the QCP picture. This discovery reveals the originality that is intimately related to the unconventional superconducting mechanism.

We appreciate the critical reading and constructive suggestions from Greg Stewart, and useful discussions with Tao Xiang and Qimiao Si. This work is supported by the Ministry of Science and Technology of China (973 Projects No. 2011CBA00102, No. 2010CB923002, and No. 2012CB821403), the NSF of China, NCET project, and PAPD. Work at Brookhaven was supported by DOE through Contract No. DE-AC02-98CH10886.

[1] I. I. Mazin, D. J. Singh, M. D. Johannes, and M. H. Du, Phys. Rev. Lett. **101**, 057003 (2008).

[2] K. Kuroki, S. Onari, R. Arita, H. Usui, Y. Tanaka, H. Kontani, and H. Aoki, Phys. Rev. Lett. **101**, 087004 (2008).

[3] C. Cao, P. J. Hirschfeld, and H.-P. Cheng, Phys. Rev. B **77**, 220506 (2008).

[4] F. Wang, H. Zhai, Y. Ran, A. Vishwanath, and D.-H. Lee, Phys. Rev. Lett. **102**, 047005 (2009).

[5] C. Fang, H. Yao, W. F. Tsai, J. P. Hu, and S. A. Kivelson, Phys. Rev. B **77**, 224509 (2008).

[6] Q. Si and E. Abrahams, Phys. Rev. Lett. **101**, 076401 (2008).

[7] F. Krüger, S. Kumar, J. Zaanen, and J. van den Brink, Phys. Rev. B **79**, 054504 (2009).

[8] K. Haule, J. H. Shim, and G. Kotliar, Phys. Rev. Lett. **100**, 226402 (2008).

[9] G. Mu, H. Luo, Z. Wang, L. Shan, C. Ren, and H.-H. Wen, Phys. Rev. B **79**, 174501 (2009).
[10] F. Hardy, P. Burger, T. Wolf, R. A. Fisher, P. Schweiss, P. Adelmann, R. Heid, R. Fromknecht, R. Eder, D. Ernst, H. v. Löhneysen, and C. Meingast, Europhys. Lett. **91**, 47008 (2010).
[11] P. Popovich, A. V. Boris, O. V. Dolgov, A. A. Golubov, D. L. Sun, C. T. Lin, R. K. Kremer, and B. Keimer, Phys. Rev. Lett. **105**, 027003 (2010).
[12] S. L. Bud'ko, N. Ni, and P. C. Canfield, Phys. Rev. B **79**, 220516 (2009).
[13] J. S. Kim, B. D. Faeth, and G. R. Stewart, Phys. Rev. B **86**, 054509 (2012).
[14] J. S. Kim, G. R. Stewart, S. Kasahara, T. Shibauchi, T. Terashima, and Y. Matsuda, J. Phys.: Condens. Matter **23**, 222201 (2011).
[15] S. L. Bud'ko, D. Y. Chung, D. Bugaris, H. Claus, M. G. Kanatzidis, and P. C. Canfield, Phys. Rev. B **89**, 014510 (2014).
[16] V. G. Kogan, Phys. Rev. B **80**, 214532 (2009).
[17] B. Shen, H. Yang, Z. S. Wang, F. Han, B. Zeng, L. Shan, C. Ren, and H. H. Wen, Phys. Rev. B **84**, 184512 (2011).
[18] J. Zaanen, Phys. Rev. B **80**, 212502 (2009).
[19] B. Zeng, B. Shen, H. Luo, G. Mu, P. Cheng, H. Yang, L. Shan, C. Ren, and H.-H. Wen, Phys. Rev. B **85**, 224514 (2012).
[20] Z. Xu, J. Wen, G. Xu, Q. Jie, Z. Lin, Q. Li, S. Chi, D. K. Singh, G. Gu, and J. M. Tranquada, Phys. Rev. B **82**, 104525 (2010).
[21] J. Hu, T. J. Liu, B. Qian, A. Rotaru, L. Spinu, and Z. Q. Mao, Phys. Rev. B **83**, 134521 (2011).
[22] V. Tsurkan, J. Deisenhofer, A. Günther, C. Kant, M. Klemm, H.-A. K. von Nidda, F. Schrettle, and A. Loidl, Eur. Phys. J. B **79**, 289 (2011).
[23] T. Klein, D. Braithwaite, A. Demuer, W. Knafo, G. Lapertot, C. Marcenat, P. Rodière, I. Sheikin, P. Strobel, A. Sulpice, and P. Toulemonde, Phys. Rev. B **82**, 184506 (2010).
[24] A. Günther, J. Deisenhofer, C. Kant, H-A. K. von Nidda, V. Tsurkan, and A. Loidl, Supercond. Sci. Technol. **24**, 045009 (2011).
[25] J.-Y. Lin, Y. S. Hsieh, D. A. Chareev, A. N. Vasiliev, Y. Parsons, and H. D. Yang, Phys. Rev. B **84**, 220507 (2011).
[26] U. Stockert, M. Abdel-Hafiez, D. V. Evtushinsky, V. B. Zabolotnyy, A. U. B. Wolter, S. Wurmehl, I. Morozov, R. Klingeler, S. V. Borisenko, and B. Büchner, Phys. Rev. B **83**, 224512 (2011).
[27] F. Wei, F. Chen, K. Sasmal, B. Lv, Z. J. Tang, Y. Y. Xue, A. M. Guloy, and C. W. Chu, Phys. Rev. B **81**, 134527 (2010).
[28] F. Y. Wei, B. Lv, Y. Y. Xue, and C. W. Chu, Phys. Rev. B **84**, 064508 (2011).
[29] K. Gofryk, A. S. Sefat, E. D. Bauer, M. A. McGuire, B. C. Sales, D. Mandrus, J. D. Thompson, and F. Ronning, New J. Phys. **12**, 023006 (2010).
[30] A. K. Pramanik, M. Abdel-Hafiez, S. Aswartham, A. U. B. Wolter, S. Wurmehl, V. Kataev, and B. Büchner, Phys. Rev. B **84**, 064525 (2011).
[31] T. Noji, M. Imaizumi, T. Suzuki, T. Adachi, M. Kato, and Y. Koike, J. Phys. Soc. Jpn. **81**, 054708 (2012).
[32] K. Gofryk, A. B. Vorontsov, I. Vekhter, A. S. Sefat, T. Imai, E. D. Bauer, J. D. Thompson, and F. Ronning, Phys. Rev. B **83**, 064513 (2011).
[33] See Supplemental Material at http://link.aps.org/supplemental/10.1103/PhysRevB.89.140503 for the raw data and the fit to the normal state value of specific heat of the ten measured samples, and the entropies for the four optimally doped samples.
[34] For a superconductor with nodal gaps, there is a residual term of the specific heat coefficient due to the impurity scattering effect. This should not be the case in our present samples.
[35] Y. Zheng, Y. Wang, F. Hardy, A. E. Böhmer, T. Wolf, C. Meingast, and R. Lortz, Phys. Rev. B **89**, 054514 (2014).
[36] J. G. Storey, J. W. Loram, J. R. Cooper, Z. Bukowski, and J. Karpinski, Phys. Rev. B **88**, 144502 (2013).
[37] D.-J. Jang, A. B. Vorontsov, I. Vekhter, K. Gofryk, Z. Yang, S. Ju, J. B. Hong, J. H. Han, Y. S. Kwon, F. Ronning, J. D. Thompson, and T. Park, New J. Phys. **13**, 023036 (2011).
[38] H.-H. Wen, Rep. Prog. Phys. **75**, 112501 (2012).
[39] J. S. Kim, E. G. Kim, G. R. Stewart, X. H. Chen, and X. F. Wang, Phys. Rev. B **83**, 172502 (2011).
[40] F. L. Ning, K. Ahilan, T. Imai, A. S. Sefat, M. A. McGuire, B. C. Sales, D. Mandrus, P. Cheng, B. Shen, and H.-H. Wen, Phys. Rev. Lett. **104**, 037001 (2010).
[41] T. Shibauchi, A. Carrington, and Y. Matsuda, Annu. Rev. Condens. Matter Phys. **5**, 113 (2014).
[42] S. E. Sebastian, N. Harrison, M. M. Altarawneh, C. H. Mielke, R. Liang, D. A. Bonn, and G. G. Lonzarich, Proc. Natl. Acad. Sci. USA **107**, 6175 (2010).
[43] P. Coleman, C. Pépin, Q. Si, and R. Ramazashvili, J. Phys.: Condens. Matter **13**, 723 (2001).